Phase Behavior of a Binary Lipid Shortening System: From Molecules to Rheology

K.L. Humphrey, P.H.L. Moquin, and S.S. Narine*

Department of Agricultural, Food and Nutritional Science, Agri-Food Materials Science Centre, University of Alberta, Edmonton, Alberta, Canada T6G 2P5

ABSTRACT: The phase behavior of fully hydrogenated canola oil in soybean oil was investigated using iso-solid lines from temperature-controlled pulse-NMR along with DSC data, with the rate of cooling of crystallized samples kept constant. The molecular diversity within the fat system was investigated using HPLC and GC. The microstructure of the fats was determined using a temperature-controlled polarized light microscope, and the polymorphism of the solidified fat structures was determined *via* a temperature-controlled X-ray diffractometer. Hardness was measured by a temperature-controlled Instron mechanical analyzer with a penetration cone. The phase behavior predicted by the DSC and iso-solid lines did not account for the hardness trends observed, as the microstructure and polymorphism of the fat also played a significant role. The addition of hard fat to a system did not consistently increase the hardness of the fat system. Furthermore, the solution behavior demonstrated by the iso-solid line diagram did not account for all trends in melting behavior, as both intersolubility and polymorphic changes occurred simultaneously. It was found that variations in hardness can be inferred from structural changes, although the structural level causing variation differs.

Paper no. J10635 in *JAOCS 80,* 1175–1182 (December 2003).

KEY WORDS: Crystallization, crystal network, fats, phase behavior, rheology, shortening.

A phase is a domain, homogenous with respect to chemical composition and physical state (1). A natural fat is an example of a system of coexisting homogeneous domains in equilibrium. The relationship and occurrence of phase change in a fat system is referred to as the phase behavior of the fat. Phase behavior, characterized by the study of the solid fat content (SFC), is important in optimizing production processes and maintaining production quality, and has been used to predict important attributes such as mouthfeel and hardness in fat-containing food products. Studies on phase behavior also lead to a better understanding of the ways in which fat blends interact—an important understanding, because the large-scale industrial production of shortenings and other fat-containing products often requires blending of lipids from many different sources.

The use of iso-solid lines to characterize phase behavior is important in illustrating some aspects of intersolubility but is ultimately limited in scope. In many instances, iso-solid line behavior may not indicate changes in polymorphism of the samples and certainly does not impart information beyond the prediction of hardness by SFC, a method that has been shown to be imperfect (2–4). On the other hand, DSC phase measurements can reflect changes in polymorphism as well as intersolubility. However, such changes are not attributable to either polymorphic or intersolubility effects alone when utilizing purely DSC data. Therefore, it is important to study phase behavior by using a number of different techniques, such as X-ray diffraction (XRD; 5), microstructure analysis, GC, and cone penetrometry.

The fat systems used in this study are mixtures of fully hydrogenated canola and soybean oils. These two lipids were selected for study because they form a solution that has yet to be studied and they provide a good complement of TAG. In North America, both of these oils are easily obtainable and economical. Furthermore, there is a potential demand for the use of hard canola in soybean oil as shortening due to the low *trans*-FA content, which would comprise a healthier consumer product.

The purpose of this study is to establish a relationship between the phase behavior, structural network, and mechanical properties of the canola–soybean lipid system and to provide a methodology to study similar shortening systems.

EXPERIMENTAL PROCEDURES

When referring to sample holding temperature as well as cooling and heating rates, all temperatures are reported to a certainty of ±0.5°C.

Sample preparation. Fully hydrogenated canola was mixed with nonhydrogenated soybean oil at dilutions ranging from 0 to 100% (w/w) canola in 5% increments. Jars containing fat mixtures were tightly covered and stored at −5°C to minimize autoxidation. Each fat mixture was completely melted by heating to 90°C before being stirred for 2 min using a mechanical stirrer. Three samples of approximately equal mass were prepared for each measurement technique. The samples were tempered by equilibrating the sample at 90°C for 5 min and then cooling to 15°C at a rate of 10°C/min. The samples were stored at 15°C, and all instruments were temperature controlled at 15°C. The XRD tubes were filled with sample from the Instron pans 48 h after tempering.

NMR. The instrument used in the investigations was a Bruker minispec mq SFC analyzer (Milton, Ontario, Canada), which is a pulse magnetic resonance spectrometer with a

*To whom correspondence should be addressed at 4-10 Agricultural/Forestry Centre, University of Alberta, Edmonton, Alberta, Canada T6G 2P5. E-mail: suresh.narine@ualberta.ca

temperature-controlled measurement chamber. The data sampling procedure was fully automated, and the SFC was calculated and displayed by computer software.

SFC measurement. The sample tubes were placed in a 15°C bath for 15 min before insertion into the NMR probe. After the SFC measurement, the sample tube was replaced into the 15°C bath. This step was repeated for all the other sample tubes, and then the temperature of the bath containing the samples was increased by 5°C and equilibrated for 15 min. Likewise, the SFC for all sample tubes was measured for temperatures ranging from 25 to 70°C. The samples were then retempered as described above. The SFC measurement was repeated, this time decreasing the temperature in 5°C increments from 15 to 0°C.

SFC analysis. Experimentally determined SFC values were used to construct iso-solid diagrams in three different ways. In the first, the averages of the actual composition results were plotted by method to construct iso-dilatation diagrams, as outlined by Rossell (6). The second method used a quadratic interpolation (7). The SFC was plotted vs. temperature for each dilution in the third method. This graph was then interpolated for temperature for a given SFC using GraphPad Prism software (San Diego, CA), and a multiple line graph of temperature vs. composition was made in which each line represented one SFC value (8). The interpolation graph is presented herein.

Crystallization onset measurement. The SFC of each NMR tube was measured for 7 min, during which time the sample was tempered as described above using a cooling system that allowed the temperature within the chamber to be decreased or increased at specific rates (9). The time at which the SFC had increased above 1% was recorded as the onset of crystallization.

DSC. The instrument used in the investigations was the DSC 2920 Modulated DSC (TA Instruments, New Castle, DE). The data sampling and temperature control procedures were fully automated and controlled by the TA Instrument Control software program, and the output spectra were analyzed with TA Universal Analysis software to find the peak maximum of crystallization and melting, as well as respective enthalpies. All samples were normalized to a uniform sample mass of 15 g.

Tempering DSC samples. The prepared pans were processed twice, first for crystallization and immediate melting of the sample, and second for crystallization with the purpose of melting after 48 h. To obtain the crystallization curve, the sample was tempered as described above. To obtain the melting curve, the sample was equilibrated for 2 min at 15°C before increasing the temperature to 90°C at 10°C/min. The melting procedure was repeated after 48 h and again after 7 d.

Hardness. The instrument used in the investigation was the Instron 4201 (Canton, MA). The software package Instron Series IX Automated Materials Tester v. 7 controlled the instrument. A 5.00 kg maximum load cell, and a steel penetration cone of mass 44.962 ± 0.0001 g were applied to a penetration depth of 8.00 mm at an angle of 31°. The position of the penetration cone was software controlled, and it was moved downward at a rate of 120.00 mm per minute with a data sampling rate of 20 points per second.

Analysis of Instron samples. Upon completion of 48 h of tempering, two measurements were taken from each pan. The slope of the displacement-force graph produced is an indication of the hardness of the sample.

XRD. A Bruker AXS X-ray diffractometer was used in this study. The procedure was automated and commanded by Bruker's General Area Detector Diffraction System v. 4.1.08 (GADDS) software with a measurement time of 450 s and a maximum display count of 127.

Microscopy. A high-resolution polarized light microscope, equipped with a Hamamatsu digital camera and a Linkam LTS 350 (Linkham Scientific Instruments, Tadworth, Surrey, United Kingdom), was used. The microscope assembly was controlled by Openlab 3.0.8 software (Improvision, Coventry, United Kingdom). Photographs were taken 15 min, 48 h, and again 7 d after tempering.

RESULTS AND DISCUSSION

All of the studied samples are solutions of many different TAG molecules, which are in motion within the sample. This motion is affected by limitations due to heat transfer and viscosity of the sample and by limits to molecular diffusivity due to conformation of the molecule. The interaction between the TAG depends on the TAG present in the solution and on the conformation of growing surfaces. If certain molecules are in the required orientation and concentration, and if an external driving force is applied to the system, then the molecules will associate to form an embryo. The driving force may be an increase in pressure or the concentration of the species leading to supersaturation, or it may be a decrease in temperature causing supercooling to occur within the system. If the embryo increases to the critical size from which growth will continue spontaneously without the continuous application of a driving force, then nucleation has occurred.

A nucleus of critical size will possess attributes of a particular polymorphic or polytypic form. The polymorphism of a sample refers to the packing arrangement assumed by the molecules within the crystals. The α polymorphic form has the lowest thermodynamic stability but also has the potential to mature into the more stable β′ or β forms (10). The nuclei formed will grow to form crystallites at the submicrometer level. The continued formation and growth of these crystals, as well as the development of the microstructure of the system, require molecules to move toward the structure at the same time as the heat of fusion disperses from the structure. As a greater percentage of the sample crystallizes, the movement of mass throughout the system is slowed owing to the increase in viscosity caused by the lack of free material within which a molecule can flow. The flow of heat also will be reduced owing to a lack of liquid oil to conduct it away from the structure. If heat is not conducted away from the structure, melting may occur. Under similar constraints, the crystallites continue to aggregate under heat and mass transfer

limitations and form microstructural elements (1–10 μm); further aggregation of such elements results in the formation of microstructures (50–140 μm) (11). The growth mode of the final structure is the collection of decisions governing structure creation to produce the final network.

Crystallization is the growth and aggregation of the nuclei into crystalline structures that can be detected with NMR, polarized light microscope, and XRD (among other) methods. After nucleation, it is possible for the molecules to re-enter the melt, for the structure to ripen, and for polymorphic changes to occur, with the events after nucleation not necessarily being sequential. The total crystallization process affects the SFC of the sample, and it is possible for two samples with the same SFC value to possess very different polymorphic forms as well as a diverse microstructure. A change in the temperature of the fat will typically cause a change in the SFC value if the change is within the melting range of the fat. However, Figure 5 *(vide infra)* shows that at 60°C the SFC is weakly temperature dependent, as it mainly depends on the relative amount of solidified saturated fat fractions from canola. Thus, a temperature change in this case has relatively little effect on the SFC value of the sample. However, the SFC of a fat sample alone does not impart information on the functional properties of a lipid network; thus, this paper undertakes further investigation into these functional properties.

As shown in Table 1, the dominant TAG in fully hydrogenated canola (SSS 79.6%) is not the same as the dominant TAG in soybean oil (LLL 12.8%). Thus, as one increases the concentration of canola by 5%, the percentage increase of the assortment of canola-contributed TAG within the sample is essentially 5%. As there are no TAG of significant proportion in common between the fully hydrogenated canola and soybean oil, one cannot draw conclusions that relate the concentration of a particular TAG to the specific microstructure assumed by the system or the functional properties it displays. However, as one increases the percentage of canola in the blend, the number of different molecules present in significant proportion decreases, because canola has fewer TAG than soybean oil. Thus, as the samples tend to 100% canola, the relative molecular diversity of each sample decreases.

Figure 1 shows the crystallization curves of each sample, as determined by DSC. A wider peak in a crystallization curve in Figure 1 implies that the final crystals will have grown from a large number of "types" of nuclei, as nucleation occurred over a longer time span. A large nucleation window may also point to the existence of an inhibitor to nucleation, whether viscosity of the sample, heat diffusion constraints, or molecular diversity. A more narrow crystallization peak suggests that all crystals within the sample nucleated at approximately the same time. This would suggest the presence of a single type of nuclei that grows into crystals. If the peak width (which indicates the temperature range over which the sample crystallizes) or the enthalpy (which is the total heat released per gram of sample) for all samples is consistently increasing, then differences between the samples with respect to onset of crystallization, polymorphism, microstructure, and SFC are not attributable to the growth mode of the crystals. Adjacent curves in Figure 1 typically vary, with respect to full-width half maximum (FWHM), by 1°C or less. The one exception to this trend is for the 45 to 50% canola samples in which a change of 4°C occurs. Thus, the growth mode of the 50% sample is not similar to the growth mode of the 45% sample, whereas this is not the case for all other neighboring samples.

TABLE 1
Relative Percentages of TAG in Soybean Oil (12) and Fully Hydrogenated Canola Oil[a] (13)

TAG	Soybean oil	Fully hydrogenated canola oil	TAG	Soybean oil	Fully hydrogenated canola oil
LLL	12.8		LSL	0.2	
LLLn	3.9		LSO	0.3	
LLnLn	0.4		LSS	0.1	
LLnO	1.7		OLnO	0.5	
LLnP	1.0		OLnP	0.6	
LLnS	0.0		OLnS	0.3	
LLO	15.6		OLO	4.6	
LLP	9.5		OLP	6.0	
LLS	3.7		OLS	2.3	
LnLLn	0.3		OOO	1.6	
LnLnO	0.3		OOP	2.1	
LnLnP	0.1		OOS	0.8	
LnLnS	0.1		OPO	0.2	
LnLO	2.5		OPP	0.3	
LnLP	1.4		OPS	0.1	
LnLS	0.5		OSO	0.1	
LnOL	1.3		OSP	0.1	
LnOLn	0.1		PLnP	0.2	
LnOO	0.8		PLnS	0.1	
LnOP	0.5		PLP	1.7	
LnOS	0.2		PLS	1.3	
LnPL	0.2		POP	0.6	
LnPO	0.1		POS	0.5	
LnPP	0.1		PPL	0.2	
LnSL	0.1		PPP	0.1	Negligible
LOL	4.4		PPS	0.1	0.5
LOO	5.3		PSP		0.5
LOP	3.3		PSS		16.3
LOS	1.3		SLS	0.3	
LPL	0.5		SOS	0.1	
LPO	0.7		SPS		0.2
LPS	0.2		SSS		79.6
			Others	0.5	2.9

[a]Abbreviations: L, linoleic; Ln, linolenic; O, oleic; P, palmitic; S, stearic.

Figure 2 shows the onset time of crystallization as it varies with the composition of the solution. The systematic error is ±20 s as a result of the difficulties associated with obtaining the measurements at the 10°C/min cooling rate. Nevertheless, as the amount of canola in the melt increases, the time at which the induction of crystallization occurs also decreases with no significant deviations from the trend. This is expected, as one increases the amount of fully hydrogenated canola, which crystallizes at a higher temperature than soybean oil, and the sample's onset time decreases.

The melting behavior for each sample, illustrated by the enthalpy of melt curve, is shown in Figure 3. Changes in the shape of the enthalpy curves are due to the variances in polymorphic structure assumed by the sample. There is a steady

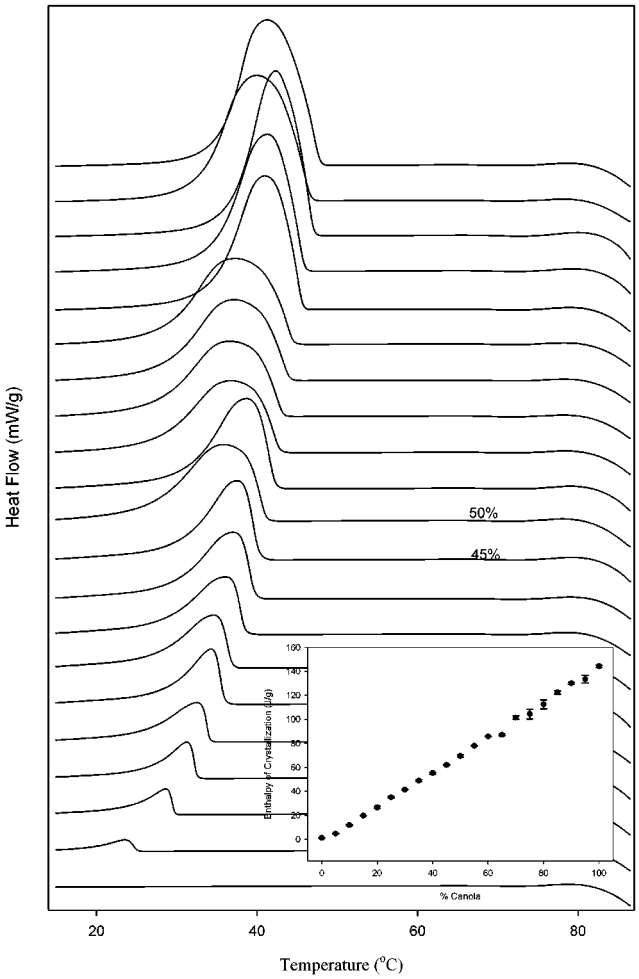

FIG. 1. Crystallization heat flow vs. temperature. Inset: enthalpy of crystallization vs. composition. Each curve represents the heat flow during the cooling process for a sample. The 0% canola sample is the bottommost curve on the graph, and the percent canola composition of the samples increases by 5% for each subsequent curve to the 100% canola sample at the top of the graph.

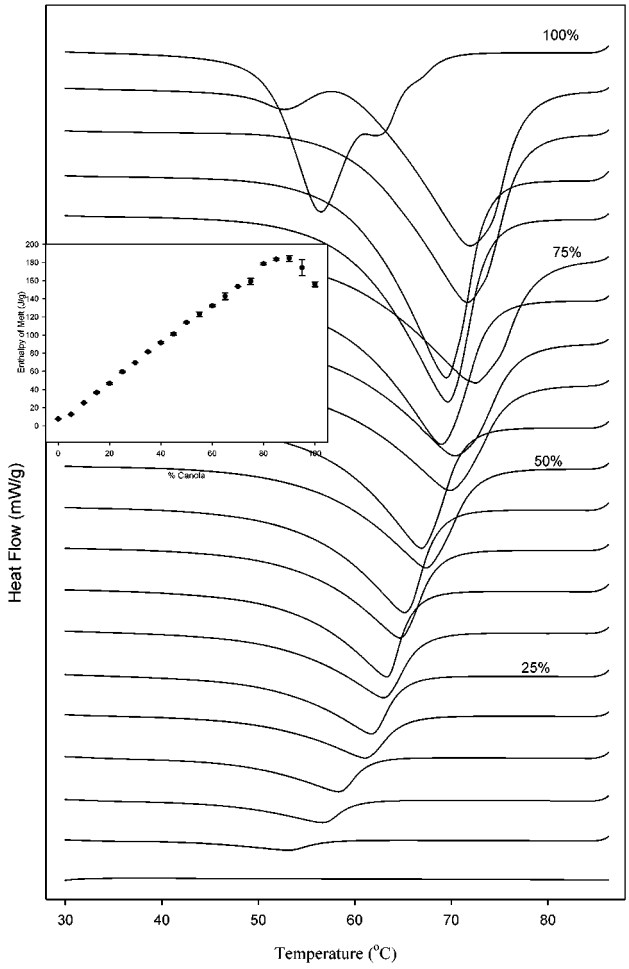

FIG. 3. Melting heat flow vs. temperature after 48 h. Inset: enthalpy of melting vs. composition curve. Each curve represents the heat flow during the melting process for a sample. The 0% canola sample is the bottommost curve on the graph, and the percent canola composition of the samples increases by 5% for each subsequent curve to the 100% canola sample at the top of the graph.

increase in the location of the melting peak maximum for the 5 to 65% canola solutions. One would expect these samples to be of similar polymorphic form. A new trend in peak maxima occurs for the 70 to 95% samples as the peaks become narrower, with the maxima starting a new increasing trend beginning lower than the peak maximum of the 65% canola blend. Clearly, for these samples, the polymorphic form is different from that for the 5 to 65% samples. The 95% canola blend has a unique type of melting behavior, as the curve has a shoulder occurring at a lower temperature than the main peak. The melting behavior exhibited by the 100% canola sample is unique, as the enthalpy curve is characterized by a shoulder peak at a higher temperature than the main peak, with the maximum value at a lower temperature (57°C) than all but the 5 and 10% samples. Therefore, unique polymorphic forms are associated with the 95 and 100% canola samples.

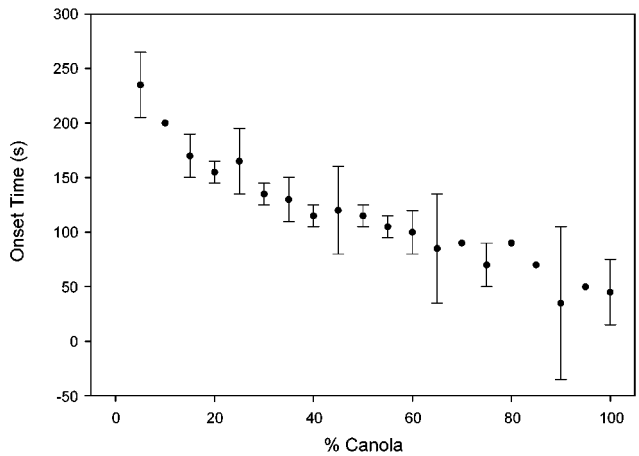

FIG. 2. Crystallization onset time. Error bars represent SD (n = 3).

Figure 4 shows an increasing hardness trend as the percentage of canola increases. The first three values, corresponding to the 5, 10 and 15% canola blends, are not zero but have very small values ($3.3 \times 10^{-5} \pm 4 \times 10^{-6}$, $3.6 \times 10^{-5} \pm 2 \times 10^{-5}$, and $6.4 \times 10^{-5} \pm 2 \times 10^{-5}$ kgf/mm). The 0% canola sample was not tested for hardness as it consisted entirely of soybean oil. Fluc-

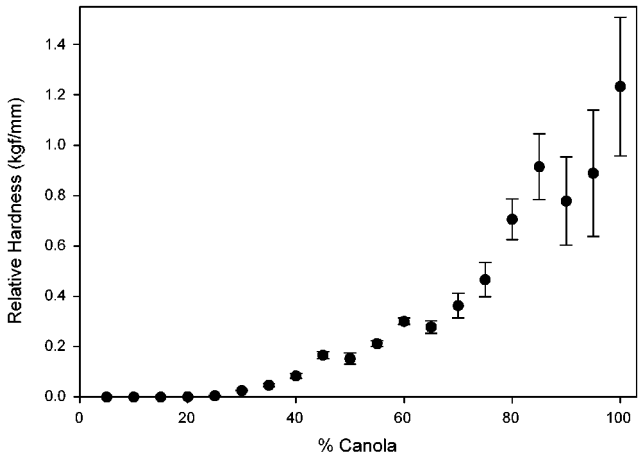

FIG. 4. Variation of hardness with composition. Error bars represent SD ($n = 3$).

tuations, where the fat sample with a higher percentage of canola exhibited a smaller slope during the hardness measurement, occurred at the 50, 65, and 90% canola mixtures.

The deviation in Figure 4 at 50% canola is mirrored by inconsistencies in Figures 1 and 3. In Figure 1, one can see that the crystallization curve for the 45% solution has a steeper onset to its peak and a narrower peak than the 50% curve. Thus, much of the crystallization and initial nucleation occurs simultaneously. This suggests good intersolubility between the hard canola and soybean oil, leading to the formation of single molecular compounds rather than a distribution of molecular compounds and therefore nuclei. Likewise, the FWHM of the crystallization curve for the 50% sample is much greater than that for the 45% canola blend (i.e., 9.35 compared to 6.23°C). This would lead one to believe that the crystallization of the 45% sample occurs within a relatively short time compared to the crystallization for the 50% canola sample. This relatively longer crystallization event would correspond to a situation in which nucleation occurs over a wider time span. Such a time span would allow a variety of nuclei, related to the existence of a number of different molecular compounds due to the solution behavior, to grow and would result in less crystal growth and more nucleation sites. Thus, in the 50% sample, there are many small structures instead of the large ones found in the 45% sample (one can see this reflected in the microstructure, to be discussed shortly). Also, in Figure 3, there is a deviation in the trend of increase in location of the melting peak maximum for 5–65% blends at the 50% canola sample, indicating a change in melting behavior between the 45 and 50% blends (i.e., a polymorphic change).

Unlike the deviation in the trend in hardness at 50% canola, the deviations in Figure 4 at 65 and 90% canola content are not due to the growth mode of the network. The curves in Figure 1 are quite similar (for the 60, 65, and 70% blends as well as the 85, 90, and 95% blends), suggesting the microstructures formed in these samples have been subjected to the same dynamics of heat and mass transfer. Thus, the deviations in the hardness curve at 65 and 90% are not due to intersolubility effects alone. The curves for enthalpy of melting in Figure 3 are also similar for the 60, 65, and 70% blends as well as the 85, 90, and 95% blends. Thus, deviations in Figure 4 at 65 and 90% are not due to growth mode selection or melting behavior of the samples.

The iso-solid line diagram constructed from the SFC of each of the fat samples is shown in Figure 5. The points sharing the same SFC value are connected using an iso-solid line. The iso-solid line at the very top of the figure is the zero SFC line. From the zero SFC line, the percentage of solid increases from left to right in 5% increments. It is evident that as the temperature and percentage of hydrogenated canola increase, the iso-solid lines converge to the right. The shape of each iso-solid line is similar to that of the neighboring lines with the slope of the iso-solid lines appearing to be similar. The iso-solid diagram also shows that a shortening made using fully hydrogenated canola and soybean oils can have a 20% SFC at temperatures between 30 and 60°C when hydrogenated canola is between 20 and 50%. It also shows that at temperatures above 55°C, temperature variation must be carefully controlled, as SFC varies greatly with temperature above this point. Figure 5 does not impart information as to the hardness of each sample as the deviations shown in Figure 4 are not seen here.

The phase changes caused by a change in the polymorphism between different fat blends can be measured with XRD. A change in the peak shape or position is indicative of a change in the polymorphism. Figure 6 shows the XRD spectra for all samples with 15% or more canola. Those samples with less than 15% were not measured due to difficulties in creating the requisite sample tubes. Two peak regions exist on each curve. The leftmost area imparts information on the polymorphic form of the crystals within the sample (the so-called short spacing); the wider peaks on the right side of the curve may be due to secondary reflections or to the polytype of the fat. The peak shapes shown on the left side of the curves in Figure 6 can be divided into four categories (A, B, C, AC). These categories are based solely on the positions and shapes of the peak as cataloged in Table 2. Within each

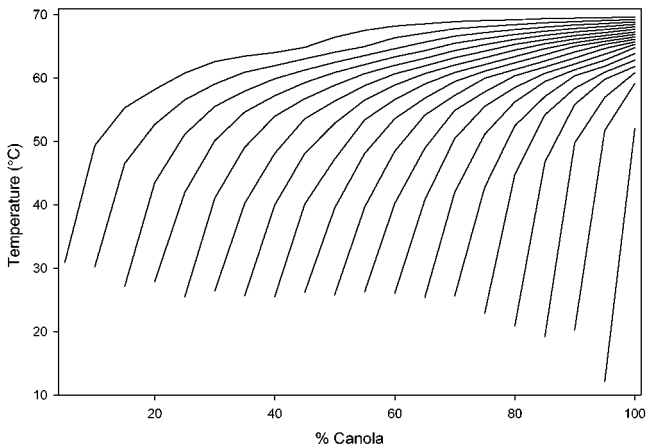

FIG. 5. Iso-solid lines created by using the interpolation method. Each curve connects points with a common solid fat content (SFC) value. The leftmost curve is the 5% SFC line, with the percentage of SFC increasing in 5% increments as one moves right on the graph.

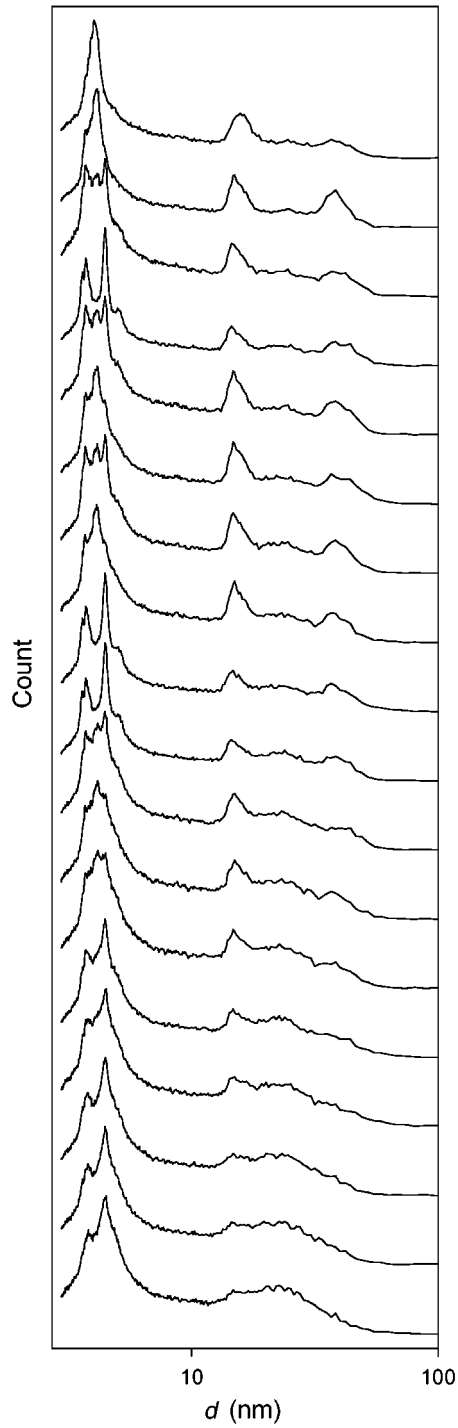

FIG. 6. X-ray diffraction curves vs. *d*. Each curve is a diffraction spectrum for a specific sample composition. The bottommost curve is the 15% canola blend, and the percentage of canola increases by 5% for each curve above. The uppermost curve is the spectrum obtained for the 100% canola sample.

category, different values of *d* are present as shown by Table 3, and these can be associated quantitatively with the possible polymorphic forms that have been defined for lipids. The α polymorphic form has a *d* value of 0.42 nm, the β′ *d* value is within the range of 0.42 to 0.43 and 0.37 to 0.40 nanometers, and the β form has a *d* value of 0.46 nm (10).

TABLE 2
Classification of X-Ray Diffraction Curves by Shape

% Canola	Classification	% Canola	Classification
100	A	45	AC
95	A	40	AC
90	B	35	C
85	C	30	C
80	B	25	C
75	AC	20	C
70	B	15	C
65	AC	10	N/A[a]
60	C	5	N/A
55	C	0	N/A
50	B		

[a]Not available.

The 100% canola peak is a well-defined single peak (Fig. 6). At 95% canola content a shoulder appears on the main peak. Further decreases in the amount of canola in the sample lead to the appearance of two to three peaks on the left side of the XRD curve. For the lowest percentages (15–35%) of canola, the peak shape is large and well-defined, with a smaller shoulder peak on the left side. The rightmost peak on the curve is not well defined at lower concentrations of canola. At 40% canola, a peak is identifiable and this becomes more apparent with increasing canola content. At 65% canola, a second, smaller peak still further right on the curve becomes evident and at 95% canola these two peaks are of the same size, with the rightmost peak disappearing in the spectrum for the 100% canola sample.

A second peak on the right side of the XRD curves in Figure 6 for the 70 to 95% canola blends corresponds to the new trend in peak maxima in Figure 3 where the peaks become narrower, with the maxima starting a new increasing trend beginning lower than the peak maximum of the 65% canola blend. In Figure 3, the unique melting curve of the 95% canola blend is possibly due to a polymorphic change, as seen by the presence of a distinct second peak on the right side of the curve in Figure 6. Again, the unique behavior of the 100% canola sample may be due to the polymorphism of the sample, as the second peak on the right side of the curve in Figure 6 is not present.

The polymorphic data evidenced by the XRD curves also assist in explaining the deviations in Figure 4. From Figure 6 one can see the difference in polymorphic character with the curve for the 45% canola blend is of type ½ A, ½ C whereas the 50% canola sample is of type B. These changes in polymorphism also contribute to the variation in hardness and support the difference in solution behavior proposed above. Also, the

TABLE 3
Average *d* Value for Each Class of X-Ray Diffraction Curves

Class	Average *d* values (nm)			
A	0.406		1.541	3.510
B	0.373	0.446	1.473	3.891
C	0.379	0.443	1.621	
AC	0.374	0.438	1.469	3.740

polymorphisms of the 60 and 65% samples differ, as shown by the XRD curves. The curve for the 60% solution is of type C and that for the 65% canola blend is ½ A, ½ C. Thus, the hardness variations are due to the differences in the packing of molecules between the 60 and 65% canola samples. For the third deviation at the 90% blend, the polymorphisms of the samples differ as shown by Figure 6. The curve for the 85% solution is of type C and that for the 90% canola blend is type B.

Figure 7 illustrates the microstructure of selected mixtures of fully hydrogenated canola oil and soybean oil. Except for minor deviations such as the placement of structures, the microstructures of the samples are alike with two exceptions. In the 50% canola blend (Fig. 7c), the structures appear smaller (≈100 μm) than those for the other solutions shown (average ≈ 500 μm). In the 50% canola sample, the structures are not closely packed and have spaces between them (≈10 μm). The other samples exhibit a close-packed arrangement, as seen in the 45% canola sample (Fig. 7b). The 80 and 85% canola samples (Figs. 7e,f), although having the same crystal size as the 90 and 95% samples (Figs. 7g,h), are also more densely packed than those in the 90 and 95% samples, as seen by the appearance of well-defined Maltese crosses, which indicate that these samples contain well-defined spherulites.

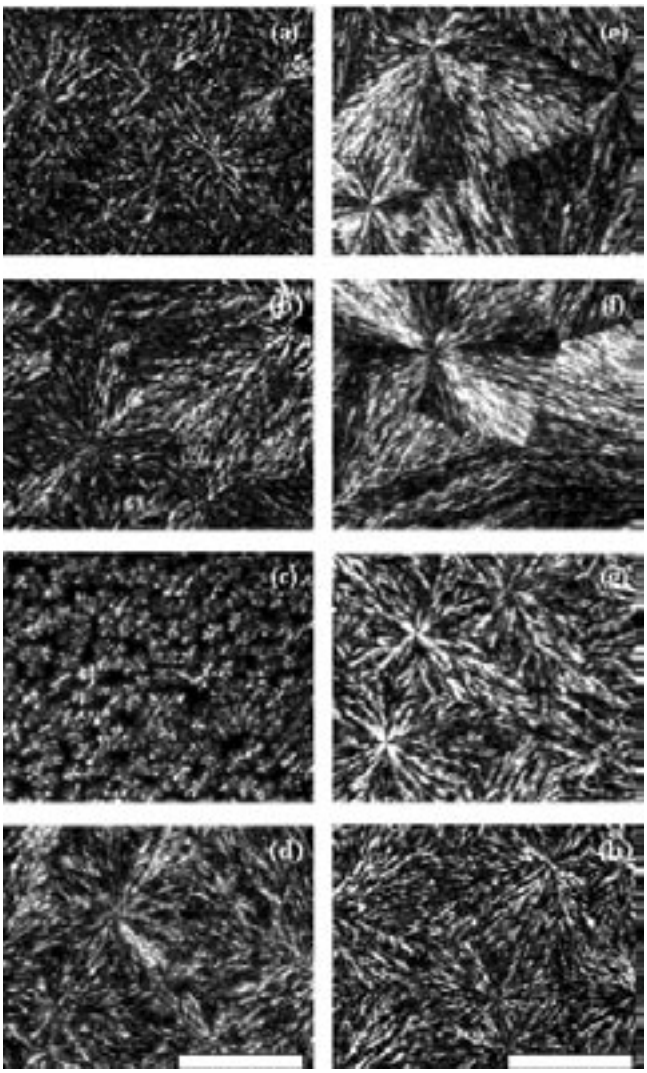

FIG. 7. Composite diagram of the microstructure of selected samples after 48 h. The samples vary with respect to percent canola content: (a) 40%, (b) 45%, (c) 50%, (d) 55%, (e) 80%, (f) 85%, (g) 90%, and (h) 95% (bar = 500 μm).

The deviation in increasing hardness (Fig. 4) at the 50% canola solution is due to the microstructure assumed as well as to polymorphism and intersolubility. In Figure 7, one can see that the sample with 50% canola is characterized by structures that are approximately 100 μm in diameter with large (~10 μm) spaces in between the structures. The other samples shown have large, closely packed structures approximately 500 μm in diameter. Note that these structures are clearly aggregates of microstructural elements, which are themselves aggregates of crystals. Thus, one can expect that under pressure from an Instron cone, the 50% sample will simply compress, with structures filling the spaces, whereas there is no room for similar compression in the 45% sample.

The deviation from the trend in the hardness curve (Fig. 4) at the 65% canola blend solution is not due to the microstructure assumed. All of the samples have a close-packed network of structures approximately 500 μm in diameter. Thus, the variation in the hardness graph is not due to the microstructure of the samples.

The deviation from the trend in the hardness curve at the solution of 90% canola is due to changes in microstructure as well as polymorphism (as seen in Fig. 6). The changes in microstructure can been seen in Figure 7; the 85 and 90% blends have the same crystal size, but the 85% canola sample is more densely packed and demonstrates greater spherulitic behavior, as suggested by the well-defined Maltese crosses that indicate the presence of well-defined spherulites.

Therefore, iso-solid lines created with SFC data do not predict the final physical properties of a lipid network. The deviations in hardness found can be explained *via* the use of intersolubility, growth mode, polymorphic, and microstructure arguments.

ACKNOWLEDGMENTS

We would like to thank Archer Daniel Midland (Decatur, IL), Bunge Foods (White Plains, NY), and National Sciences and Engineering Research Council of Canada for financial support for the research as well as Ereddad Kharraz, who performed DSC, microscope, and hardness measurements, and Kevin Pocklington, who performed XRD measurements and assisted with sample preparation.

REFERENCES

1. Moore, W.J., States of Matter, in *Basic Physical Chemistry*, Prentice-Hall, Englewood Cliffs, NJ, 1983, pp. 27–28.
2. Narine, S.S., and A.G. Marangoni, Relating Structure of Fat Crystal Networks to Mechanical Properties: A Review, *Food Res. Int. 32*:227–248 (1999).
3. Narine, S.S., and A.G. Marangoni, Factors Influencing the Texture of Plastic Fats, *inform 10*:565–570 (1999).
4. Narine, S.S., and A.G. Marangoni, Microscopic and Rheological Studies of Fat Crystal Networks, *J. Cryst. Growth 198/199*: 1315–1319 (1999).

5. Norton, I.T., C.D. Lee-Tuggnell, S. Ablett, and S.M. Bociek, A Calorimetric, NMR, and X-Ray Diffraction Study of the Melting Behavior of Tripalmitin and Tristearin and Their Mixing Behavior with Triolein, *J. Am. Oil Chem. Soc. 62*:1237–1244 (1985).
6. Rossell, J.B., Interactions of Triglycerides and of Fats Containing Them, *Chem. Ind.*:832–835 (1973).
7. Timms, R.E., Computer Program to Construct Iso-solid Diagrams for Fat Blends, *Ibid.*:257–258 (1979).
8. Rousseau, D., K. Forestiere, A.R. Hill, and A.G. Marangoni, Restructuring Butterfat Through Blending and Chemical Interesterification. 1. Melting Behavior and Triacylglycerol Modifications, *J. Am. Oil Chem. Soc. 73*:963–972 (1996).
9. Narine, S.S., and K.L. Humphrey, Extending the Capability of Pulsed NMR Instruments to Measure Solid Fat Content as a Function of Both Time and Temperature, *Ibid.* (in press).
10. Ghotra, B.S., S.D. Gyal, and S.S. Narine, Lipid Shortenings: A Review, *Food Res. Int. 35*:1015–1048 (2002).
11. Narine, S.S., and A.G. Marangoni, Structure and Mechanical Properties of Fat Crystal Networks, in *Physical Properties of Lipids*, edited by A.G. Marangoni and S.S. Narine, Marcel Dekker, New York, 2002, pp. 63–83.
12. Wang, T., Soybean Oil, in *Vegetable Oils in Food Technology: Composition, Properties, and Uses*, edited by F.D. Gunstone, CRC Press, Boca Raton, FL, 2002, pp. 21–22.
13. Neff, W.E., T.L. Mounts, W.M. Rinsch, H. Konishi, and M.A. El-Agaimy, Oxidative Stability of Purified Canola Oil Triacylglycerols with Altered Fatty Acid Compositions as Affected by Triacylglycerol Composition and Structure, *J. Am. Oil Chem. Soc. 71*:1101–1109 (1994).

[Received May 5, 2003; accepted September 10, 2003]